JOURNAL OF MATERIALS SCIENCE 8 (1973) 525–538

A study of the solid-state polymerization of trithiane

V. M. NADKARNI, J. M. SCHULTZ
Department of Chemical Engineering, University of Delaware, Newark, Delaware, USA

The temperature dependence of the rate of solid-state polymerization of trithiane was investigated in conjunction with calorimetric measurements of the heat capacity of the irradiated monomer as a function of temperature. It was found that the rate of change of entropy with temperature exhibited a maximum at about 175 °C. The curve of per cent polymerization versus isochronal, post-irradiation polymerization temperature also peaked at some 175 °C. Finally, the existence of a crystalline phase-transition in the monomer at about 194 °C was discovered by DSC and was confirmed by X-ray powder diffraction and by optical microscopy. Two models which may interrelate this set of phenomena are suggested.

1. Introduction

The field of solid-state polymerization has emerged as an active field of investigation only during the last 10 years. The broad outline of such polymerization is as follows. After initiation induced by irradiation or by chemical reaction, motion of some sort must occur within the monomer crystal lattice for the reaction to propagate. Given a set of chemical possibilities, whether or not the chain propagation reaction will occur under a given set of conditions, and also the extent of this reaction, depend, among other things, on the relationship between the reactant and the possible product structures and on whether the required mode of motion is allowable by the lattice and thermal conditions. The former of these two controlling features, the relation between crystal structure of monomer and polymer, has been an area of intensive investigation. On the other hand, it is surprising to find that relatively little effort has been made specifically to investigate the role of molecular mobility and to assess the relative importance of spatial arrangement and mobility.

For elucidating the mechanism by which the cyclic monomers link together in a long chain after bond-opening, knowledge of the crystal structure and of the crystal packing of the monomer and the corresponding polymer is essential. An understanding of the intermolecular contacts and packing density is necessary in predicting or explaining the most probable direction of propagation. This goal has greatly stimulated interest in the investigations of crystal structures of the various cyclic monomers [1-6]. Busetti *et al* have refined the crystal structure of trioxane and have utilized these results with particular regard to the molecular packing and its influence on the polymerization mechanism by which "twinned" crystals of polyoxymethylene are formed [1]. Their work has shown that polymerization occurs in the directions of the two shortest C . . . O contacts.

The sulphur analogue of trioxane, trithiane, was first reported as not undergoing radiation polymerization in the solid state. However, in 1964, Lando and Stannett reported the formation of crystalline polythiomethylene in the solid state [3, 7]. Since then the structure of trithiane has been thoroughly investigated [2, 3, 5, 6]. Trithiane molecules are known to have a chair conformation and to exhibit an orthorhombic crystal structure at room temperature. The melting point and the stability of trithiane are both high in comparison with trioxane. Mammi *et al* [8] have studied the relative orientation of the twinned polythiomethylene crystals and concluded that the solid-state polymerization of trithiane takes place in a direction normal to the *c*-axis of trithiane. The reported high packing-density of trithiane [6] may be related to the fact that irradiated crystals polymerize only by heating for many hours at relatively-high temperatures (> 160 °C), when molecular

motions and free volume are sufficient.

It is suggested that the cyclic monomers polymerize in the solid state by an ionic addition mechanism [9] on the basis of the following considerations:

(a) It has been well known that these cyclic monomers can easily polymerize only by ionic catalysts but not by radical catalysts or ultraviolet light.

(b) The polymer formed in the solid state is recognized to have just the same structure as that prepared by ionic catalyst.

(c) The polymerization of these monomers proceeds only in the solid but not in the liquid state. This may well be explained by supposing that the ions formed by radiation have a long enough lifetime for initiation of the solid state polymerization only in the solid state.

In spite of these speculative arguments, not many investigations have yet been reported as far as the general mechanisms and kinetics of solid-state polymerization of cyclic monomers are concerned, and most of the research has dealt, more or less completely, with the structural aspects of the problem. Regarding the kinetics of polymerization, a variation of polymerization rate with temperature has been reported in some instances [9, 10]. In the case of the cyclic monomer of β-propiolactone, a maximum in polymerization rate with respect to temperature has been reported [9]. Such a temperature dependence is difficult to interpret without the aid of other supporting data regarding crystal structure transitions and the extent of molecular motion in the monomer lattice. Nevertheless, the observation is interesting enough to warrant further investigation.

There are at least two thermodynamic properties which could be indirectly coupled with this problem area. Entropy and heat capacity of a substance are known to be related to the degree of disorder in the system and also to the extent of molecular motion. It therefore seems reasonable that the influence of a process variable, such as polymerization temperature, on per cent polymerization or on polymerization rate, could be understood better if studied in conjunction with a study of the variation of entropy and/or heat capacity with temperature. To this end, then, the present investigation was undertaken in order to relate the temperature dependence of per cent polymerization of cyclic monomers to the thermodynamic properties. The work discussed herein deals with the solid-state polymerization of trithiane and attempts to illustrate the interrelationship between the course of the solid-state reaction and the phenomena occurring within the monomer lattice, on the basis of thermodynamic and structural data. The choice of the particular cyclic monomer, trithiane, is one of experimental convenience and ease of handling. It is believed, however, that the general conclusion and ideas drawn from the present work would serve in arriving at generalizations for ring polymerization.

2. Experimental

2.1. Polymerization

The monomer sample used was symmetric trithiane (K and K Laboratories, m.p. 215 to 216°C). Small needle-shaped crystals of the monomer were obtained by subliming the commercial powder in a long-necked stoppered Erlenmeyer glass flask, with slow controlled heating. These vapour-grown crystals were then sealed in 10 mm diameter Pyrex tubes, under atmospheric conditions. Ten such tubes were almost half-filled with weighed amounts of the monomer. These samples received Co^{60} γ-radiation doses of up to 7 Mrad at room temperature, at a dose rate of 0.172 Mrad h^{-1}. Particular attention was paid to the positioning of the aluminium test-tube stand inside the irradiation chamber so as to ensure fairly uniform irradiation of the bulk of the sample. The post-irradiation polymerization was carried out in five constant-temperature heat-baths maintained at 160, 170, 175, 180, and 185°C for 24½ h. Corn oil was used as the heating medium. Heat-treatment was followed by quenching into water to suppress any further polymerization.

The light brown polymer was separated from the monomer by extraction with boiling chloroform, followed by filtration. The polymer was then dried and weighed. The polymer powder did not sublime even at 200°C under atmospheric pressure.

2.2. Differential scanning calorimetry

The DuPont DSC Cell, a plug-in accessory for the DuPont 900 Differential Thermal Analyzer, was used to obtain all calorimetric data. Calibration of the sample temperature for thermal lag was carried out with four materials with well-defined transition temperatures. Calibration of the calorimeter for heats of transition was performed with a heating rate of 2°C min^{-1} using tin as a standard. The heat of fusion of tin

used for calibration is 14.2 cal g^{-1}. For highest accuracy in heat-capacity determinations, a second calibration curve based on known heat capacities was established. In the work reported here, a calibration curve was constructed using 99.999% aluminium powder of 140 to 200 mesh size.

The following additional precautions were taken to ensure quality of results. In order to reduce the error introduced by the thermal lag, all runs were carried out at heating rate of 2° C min^{-1}. It is believed that heating rates above 5° C min^{-1} may introduce some error in temperature measurements. The weight distribution among the aluminium containers was found and reference containers with a weight within 0.1 mg of the weight of the corresponding sample container were used for all runs. It was observed that a perfectly flat bottom is essential for good thermal contact of the container with the platform. Particular care was therefore taken while crimping the pan and the lid together. A Perkin-Elmer crimping press was used. Crushed ice used for the cold junction was changed after every two runs. After every run the sample was weighed to check for sublimation loss.

2.3. X-ray diffraction

Nickel-filtered Cu$K\alpha$ radiation was input to a General Electric Debye-Scherrer camera (14.32 cm diameter) to obtain X-ray powder patterns. The powder samples, ground to the 400 mesh size and contained in 0.3 mm diameter capillaries, were exposed for 11½ h. Powder patterns of commercial monomer, vapour-grown monomer, solution-grown monomer (from chloroform solution) and melt-grown monomer were obtained. In addition, diffractometry was carried out on two samples of the vapour-grown monomer crystals which were annealed at 196° C for about 4 h. One of the samples was then quenched in ice-cold water, whereas the other one was allowed to cool down slowly. The reasons for these treatments will be discussed later, in connection with an observed phase transition. Both these samples were ground to the 400 mesh size and their powder patterns were obtained. Finally, to check the effect of grinding on the state of the material, two additional runs were made. A sample of vapour-grown monomer crystals, after receiving a γ-radiation dose of 7 Mrad, was ground to 400 mesh size and was subsequently exposed to the X-radiation to get the powder pattern. Also, a well-ground, 400 mesh-size sample of the monomer was subjected to a total dose of 7 Mrad of γ-radiation and then its powder pattern was obtained.

2.4. Optical microscopy

A standard polarizing microscope, equipped with a hot stage, was used. Photographs of the vapour-grown monomer crystals at different temperatures were taken at a magnification of ×600, using a Polaroid camera. The monomer sample, on the microscope slide, was covered with thin cover glass to prevent sublimation.

3. Results

3.1. Temperature dependence of polymerization rate

The extent of polymerization attained in a specific period at different temperatures can be regarded as an indirect measure of the polymerization rate at the various temperatures. More explicitly, it is the time-average rate of polymerization. In our case post-irradiation polymerization was carried out for 24½ h at five different temperatures. Specimens from two different irradiation batches were kept in each bath. The extent of polymerization was determined, knowing the weight of the polymer formed from known weight of monomer. Fig. 1 shows the resulting plots of per cent polymerization versus polymerization temperature for the two batches. The trend in the variation of solid-state polymerization rate with temperature seems apparent, though the plots for the two runs do not match exactly; the polymerization rate exhibits a maximum with respect to temperature at 175° C.

The lack of exact agreement between the numerical results of the two experimental runs may be attributed to the influence of defect concentration in the monomer lattice on polymerization rate. Though the monomer crystals for both runs were grown using the same technique, it is not possible to control the crystal size. The crystal size distribution and consequently the defect concentration may therefore vary, and this could account for the observed discrepancy.

3.2. Specific heat of irradiated monomer

It should be noted that, in the context of the purpose of this work, the qualitative trends in the temperature dependence of specific heat and entropy are of more importance than their

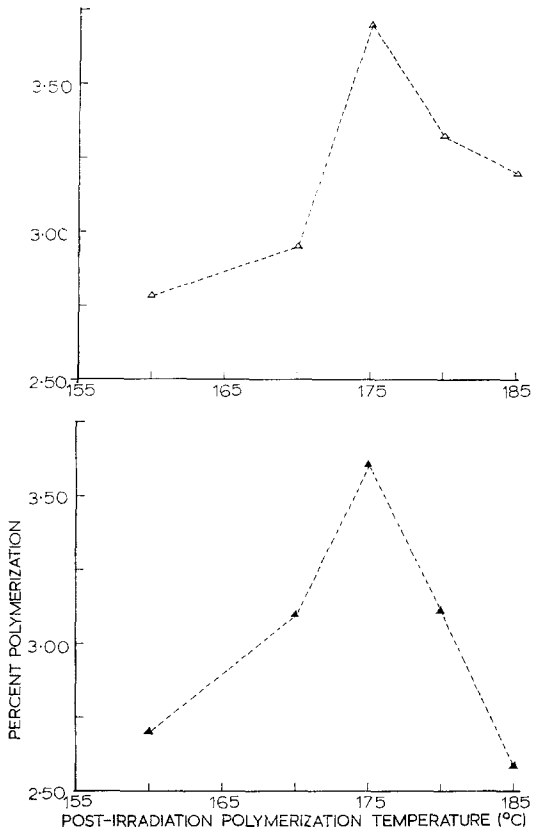

Figure 1 Temperature dependence of the extent of polymerization.

absolute numerical values. Differential scanning calorimetry (DSC) is a simple, useful technique, which is ordinarily used for arriving at such qualitative results.

Ten DSC runs were carried out with three samples of the irradiated monomer. The specific heat versus temperature data from each of these ten sets were then fitted, applying a least squares technique, to the following functional form, commonly used for representing specific heat of solids [11]:

$$C_p = P + QT + R/T^2 \qquad (1)$$

where C_p = heat capacity (cals deg^{-1} mol^{-1}); T = absolute temperature (K). The values of the constants P, Q, R were evaluated for each of the ten sets. The "average" of these ten "curves" of specific heat versus temperature was then taken by averaging the constants. The equation of the average curve is given by,

$$\hat{C}_p = \hat{P} + \hat{Q}T + \hat{R}/T^2 \qquad (2)$$

where
$$\hat{P} = \sum_{i=1}^{10} P_i/10 = 98.82$$
$$\hat{Q} = \sum_{i=1}^{10} Q_i/10 = -0.13024 \qquad (3)$$
$$\hat{R} = \sum_{i=1}^{10} R_i/10 = 6.4016 \times 10^6.$$

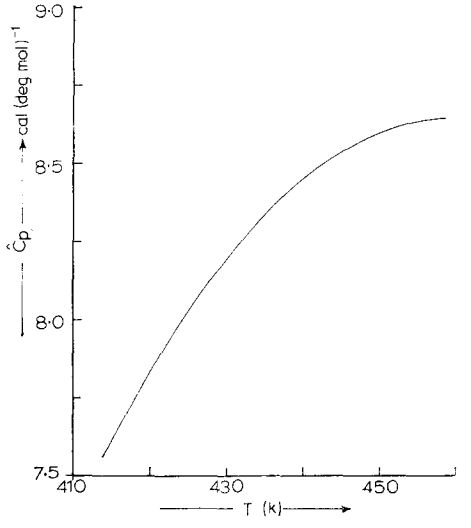

Figure 2 Variation of heat capacity with temperature.

It is important to note that Fig. 2 represents the average of "specific heat versus temperature curves", rather than average specific heat as a function of temperature; Fig. 2 is the graphical representation of Equation 2. The scatter in the specific-heat data is within $\pm$ 12.5% of the values plotted.

The entropy is related to the heat capacity by the equation,

$$dS = \frac{C_p}{T} dT \qquad (4)$$

$$\text{therefore } \frac{C_p}{T} = \frac{dS}{dT}. \qquad (5)$$

A plot of dS/dT versus temperature was thus constructed using the specific-heat data. Referring to Fig. 3, dS/dT increases initially with increasing temperature, finally passing through a maximum at around 175°C. It is interesting that the peaks in both the curves – per cent polymerization versus temperature (Fig. 1) and dS/dT versus temperature (Fig. 3) – occur at the same temperature, within experimental accuracy.

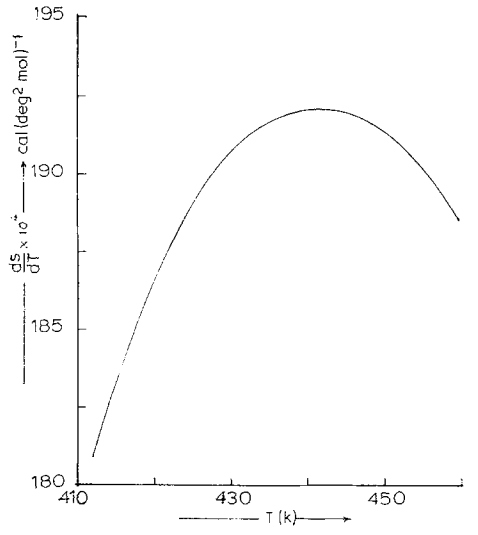

Figure 3 Effect of temperature on entropy change.

3.3. Differential scanning calorimetry

While making calorimetric measurements for the specific heat of the irradiated monomer, it was noticed that a secondary endothermic peak appears at approximately 194°C, at a temperature below that of the melting peak. A series of runs were carried out specifically to investigate this secondary peak.

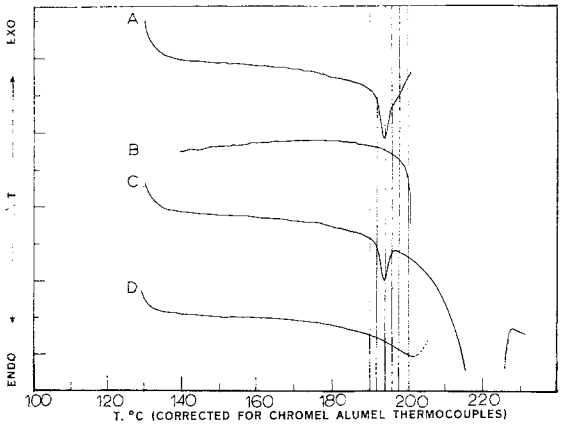

Figure 4 DSC scans of irradiated monomer.

Fig. 4 shows the results of a set of runs made with the same sample of unirradiated monomer. The monomer sample was first heated to 201°C, past the secondary peak (curve A), and subsequently air-cooled back to room temperature (curve B).* The sample was then reheated to temperatures beyond the melting point (curve C) and again cooled to room temperature in air. Curve D represents the heating of this melt-crystallized sample. Surprisingly, in this case the secondary peak near 194°C does not occur. However, if the unmelted monomer sample is heated to temperatures below the melting point and past the secondary-peak temperature, the secondary peak is fairly reproducible. This is illustrated in Fig. 5, which shows two DSC scans with the same monomer sample.

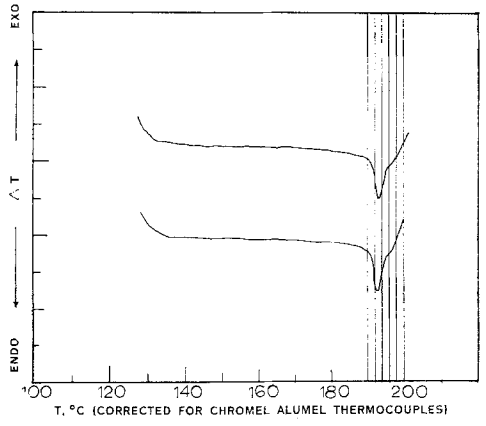

Figure 5 Reproducibility of DSC results for irradiated monomer heated to a temperature between the secondary and primary transitions.

Referring to Figs. 4 and 5, it is clear that the secondary peak is reproducible, fairly sharp and is spread over a very narrow temperature range. The peak, being endothermic, is certainly not due to the oxidation of the monomer. Also it cannot be attributed to polymerization, since solid-state polymerization reactions of ring compounds are mildly exothermic [12]. It therefore seems that the secondary peak represents some kind of solid-phase crystallographic transition.

Nevertheless, it is intriguing that the secondary peak does not appear in the cooling curve. A set of runs were performed with the same sample to investigate the cooling curves. Referring to Fig. 6, the two curves labelled H represent heating, whereas the curves labelled C represent cooling in air. The solid curves

*The initial steep portions of the curves of Figs. 4 and 5 represent a transient instrumental instability and are included in the figures to indicate the range of reliable results.

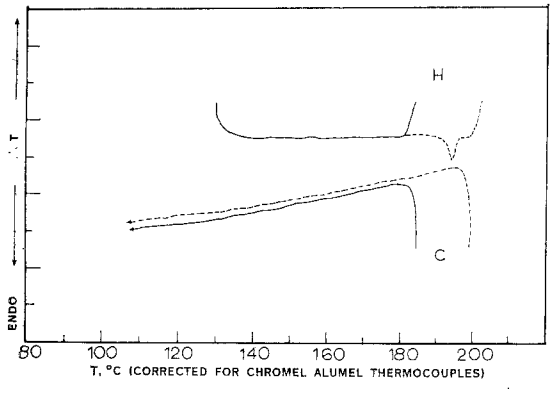

Figure 6 Effect of final-heating temperature on DSC scans taken during cooling. C and H denote heating and cooling curves. Solid and dashed lines denote first and second runs, respectively.

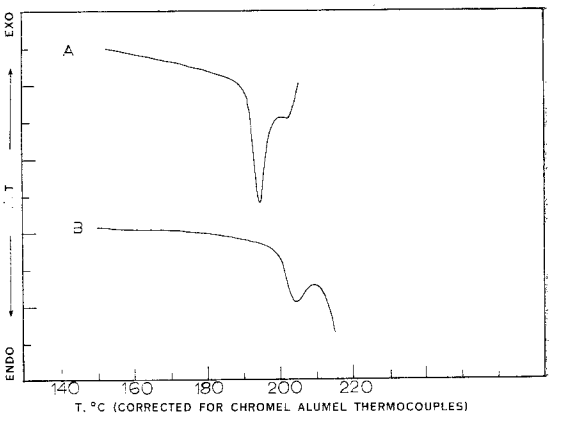

Figure 7 Effect of heating rate of the solid-state transition. Scan A taken at 10°C min^{-1}; scan B at 50°C min^{-1}. These may be compared with 2°C min^{-1} scans in Figs. 5 and 6.

correspond to the sample which was heat-treated to a temperature below the secondary peak, whereas the dotted curves correspond to the sample heat-treated to a temperature beyond the secondary peak but below the melting point. The instrument settings were the same in both these cases. These curves manifest an interesting observation that although the heating curves in the two cases overlap exactly, the dotted cooling curve lies slightly above the solid cooling curve over the entire temperature range. This fact suggests that the back-transformation from the high-temperature phase to the low-temperature phase may occur gradually over the entire cooling period.

Fig. 7 shows the DSC scans of the monomer at high heating rates. The heating rate was 10°C min^{-1} for scan A and 50°C min^{-1} for scan B; the y-axis sensitivity settings were different in the two cases. It is clear from these two curves that the secondary peak cannot be suppressed by increasing the heating rate.

The heats of transition were found by peak area measurements made from curves traced on the X-Y plotter. Fig. 8 shows a DSC scan with reversed ordinate scale. The peak areas were measured above the dotted base line. The smaller peak A represents the solid-phase transformation, while peak B is the melting peak. The results are shown in Table I. Thus the heat energy involved in the crystallographic transition is very small as compared to the heat of fusion, which is usually the case with solid-phase transformations.

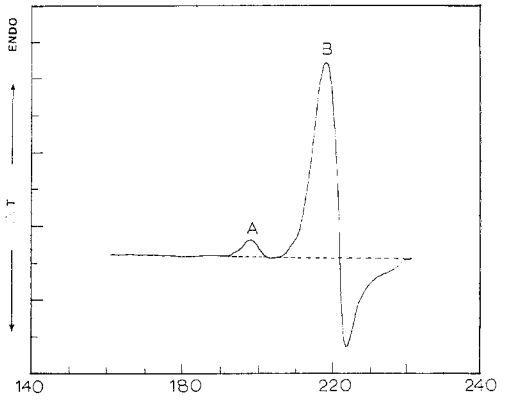

Figure 8 Determination of heats of transition (see text).

TABLE I Calorimetric data

	T (°C)	$\triangle H$(cal g^{-1})	$\triangle S$(cal K^{-1} mol^{-1})
Solid phase transformation	194	−2.603	−0.774
Melting	215	−35.400	−10.000

3.4. X-ray powder patterns

X-ray diffraction experiments were performed to confirm the existence of the solid-phase transformation and to study it in fair detail.

It was found that the commercial, solution grown, and vapour-grown samples of the monomer show exactly the same powder pattern, whereas the powder pattern of melt-crystallized monomer is slightly different. This

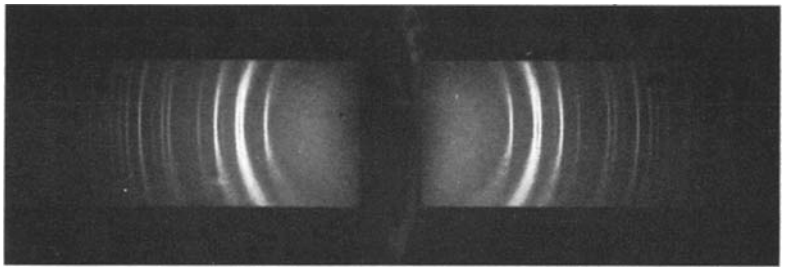

Figure 9 X-ray powder pattern of solution-grown trithiane.

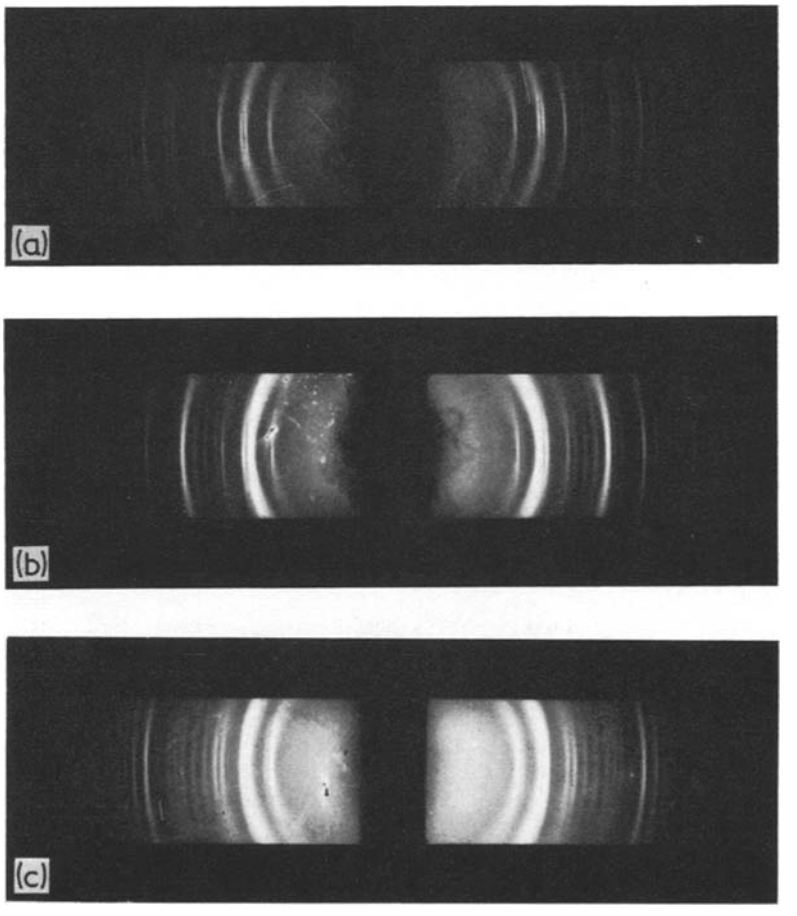

Figure 10 X-ray powder photographs of: (a) commercial trithiane, (b) quenched sample of commercial trithiane, (c) melt-crystallized trithiane.

observation seems to be consistent with the DSC results. Fig. 9 gives the powder pattern of the solution-grown monomer sample.

The quenched sample of the commercial monomer produced a powder pattern which appears to be intermediate between those of the regular commercial monomer and melt-crystallized material as illustrated in Fig. 10; patterns A, B, and C represent the commercial monomer, quenched sample of the commercial monomer and the melt-crystallized monomer respectively. A commercial monomer sample, cooled slowly from 196°C, exhibited a powder pattern similar to pattern A of Fig. 10. Both

TABLE II X-ray powder pattern analysis

Low-temperature phase (Solution-grown crystals)		High-temperature phase (Melt-grown crystals)		Quenched sample of commercial monomer	
d (Å)	Intensity	d (Å)	Intensity	d (Å)	Intensity
5.163	dark	5.175	v. dark	5.186	dark
—	—	4.926	m. dark	4.956	light
—	—	—	—	4.408	v. dark
4.330	dark	4.337	dark	—	—
4.200	dark	4.187	v. dark	4.181	dark
3.826	v.v. light	3.841	v.v. light	3.817	v.v. light
3.688	dark	3.688	dark	3.692	dark
—	—	3.549	dark	3.549	medium
3.355	light	3.362	medium	3.352	medium
—	—	3.171	medium	3.180	medium
—	—	3.019	medium	3.006	dark
2.914	medium	2.916	medium	2.916	light
2.832	medium	2.832	medium	2.825	medium
2.722	light	2.724	v. light	2.721	v. light
2.581	dark	2.581	v. dark	2.586	dark
2.458	m. dark	2.465	dark	2.459	m. dark
2.395	m. dark	2.390	medium	2.390	medium
2.329	medium	2.336	light	2.334	medium
2.295	light	—	—	—	—
—	—	2.257	v. light	—	—
2.166	light	2.173	medium	2.170	dark
2.103	light	2.106	v.v. light	2.103	light
2.058	v.v. light	2.055	v.v. light	2.060	light
2.026	v.v. light	—	—	2.026	light
—	—	—	—	1.941	light
1.916	dark	1.916	medium	1.918	light
1.770	v.v. light	1.778	medium	1.777	light
1.745	v.v. light	—	—	—	—
1.703	v. light	1.707	light	1.705	light
1.678	v. light	—	—	—	—
1.660	v. light	—	—	1.663	light
1.633	medium	1.634	v. light	1.635	light
1.622	light	—	—	—	—
1.588	dark	1.586	m. dark	1.589	dark

the quenched and slowly-cooled samples of the vapour-grown monomer were, however, found to manifest powder patterns similar to that of the regular vapour-grown material. This last result is somewhat puzzling to us.

The powder patterns were analysed to calculate the set of interplanar d-spacings for the materials. Table II gives a comparative analysis of the powder patterns of the low-temperature monomer phase (solution-grown), the high-temperature monomer phase (melt-crystallized), and the quenched sample.

The crystal structure of trithiane was first described by Moerman and Wiebenga [13]. Mammi *et al* [6] have recently redetermined accurately the crystal structure of trithiane and have reported the crystallographic data shown in Table III. Knowing the lattice dimensions of the orthorhombic trithiane cell and the spacing group, the d-spacings of the various hkl refections were calculated using the spacing formula:

$$\frac{1}{\mathrm{d}^2_{hkl}} = \frac{h^2}{a^2} + \frac{k^2}{b^2} + \frac{l^2}{c^2}. \qquad (6)$$

A comparison of the calculated d-spacings with the observed values for the low-temperature phase is shown in Table IV; the observed intensities are compared to those reported by Moerman [13]. It is clear that the experimental

TABLE III Crystallographic data of trithiane

Crystallographic system: orthorhombic Space group: $Pmn\,2_1$ (No. 31) = C_{2v}^7
$a = 7.668 \pm 0.005$ Å
$b = 7.003 \pm 0.005$ Å
$c = 5.285 \pm 0.005$ Å

results agree extremely well with the calculated values of the *d*-spacings and with the previously reported intensities of the reflections.

A comparison of the additional *d*-spacings in the powder pattern of the melt-grown monomer with the *d*-values reported by Joginder Lal [14] for the X-ray diffraction pattern of polythiomethylene revealed that these two patterns are different and confirmed that the melt-crystallized phase is truly a monomer phase and not a mixed system containing the polymer.

The powder pattern of the irradiated monomer was obtained to investigate the effect of irradiation on the crystal packing and orientation. Fig. 11 shows the patterns of unirradiated (A) and irradiated (B) samples of the vapour-grown monomer. The reflections in pattern B are sharper than those in pattern A. This effect may be attributed to a vibration-constraining effect due to the formation of dimers and trimers by irradiation. It was ascertained from the powder pattern of a sample ground before irradiation that the line sharpening effect is not due to plastic flow induced by grinding.

3.5. Optical microscopy

Photomicrographs taken during the heating and cooling of monomer crystals are shown in Figs. 12 and 13. Fig. 12 shows the vapour-grown monomer crystals at four different temperatures during the heating period, whereas Fig. 13 shows the monomer crystals at the beginning and end of the cooling period. It appears that at the transition point of about 194° C, the monomer crystals flatten out and that, when recooled, they again grow back in the direction perpendicular to the plane of the paper. This phenomenon of regaining depth is illustrated in Fig. 13.

An interesting phenomenon was observed near the transition temperature. It was invariably observed when viewing crystals as they

TABLE IV Comparison of the observed reflections with calculated *d*-spacings and reported intensities [13]

hkl	*d*-spacings (Å)		Intensities	
	Calculated	Observed	Observed	Reported
100	no reflection	—	—	—
010	7.003	—	—	—
001	no reflection	—	—	—
110	5.170	5.163	dark	m. dark
101	4.350	4.330	dark	v. dark
011	4.200	4.200	dark	dark
200	3.834	3.826	v.v. light	medium
111	3.690	3.688	dark	dark
020	3.502	—	—	—
210	3.360	3.355	light	medium
120	3.190	—	—	v.v. light
021	2.920	2.914	medium	m. dark
211	2.860	2.832	medium	m. dark
121	2.730	2.722	light	medium
002	2.643	—	—	v.v. light
220	2.590	2.581	dark	dark
012	2.470	2.458	m. dark	dark
310	2.400	2.395	m. dark	m. dark
112	2.370	—	—	v.v. light
030	2.334	2.329	medium	medium
301	2.250	2.295	light	medium
202	2.180	2.166	light	m. dark

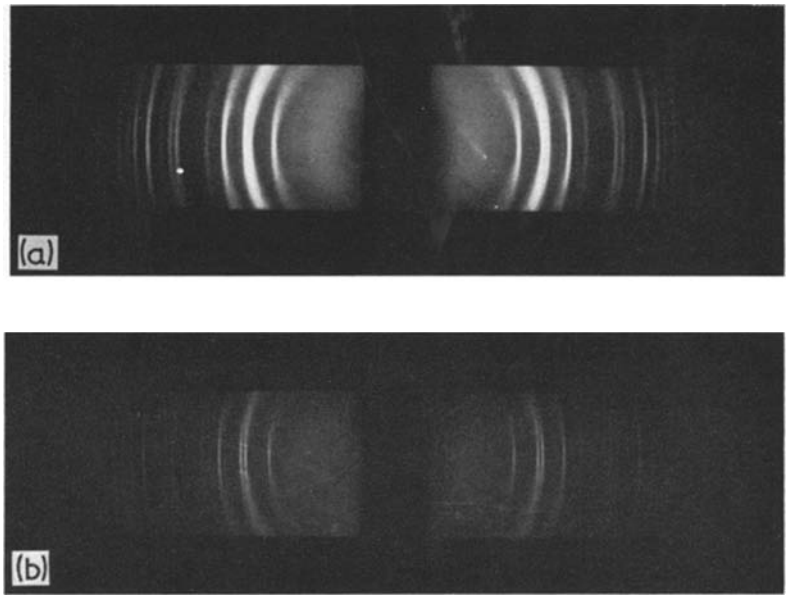

Figure 11 X-ray powder photographs of: (a) unirradiated vapour-grown trithiane, (b) irradiated vapour-grown trithiane.

are being heated on the microscope stage that in the vicinity of 194°C the whole slide becomes foggy, hindering any observation. The picture would again emerge clearly as the temperature is increased slightly.

4. Discussion

This work provides three primary pieces of information regarding the solid-state polymerization of trithiane. First, differential scanning calorimetry, supported by X-ray powder patterns, have established that trithiane undergoes a reversible phase transition near 194°C. Second, a peak in polymerization rate with temperature is observed at 175°C. Finally, a peak in the temperature dependence of dS/dT is observed, also at 175°C. A reasonable model for the interrelationship between these observations must be developed. As it happens we propose two possible models, one based directly on molecular mobility and the other based on a crystallographic transition. Further work will be necessary before a unitary model for this process can be verified.

4.1. Molecular motion, chain termination (MMCT) model

The nature of the dS/dT versus temperature curve can be explained in terms of an orientational change in the monomer lattice, involving the onset of some kind of internal motion followed by its subsequent saturation. It is supposed that at about 140° C, some mode of motion becomes "unlocked" and that the rate of entropy change with temperature increases as the temperature is increased. Subsequently, as the motion attains saturation, dS/dT begins to decrease.

Such phenomena of onset of internal motion prior to a solid phase transformation have been known to occur in many organic and inorganic compounds [15-17]. The structual observations reported [16] in the case of hexamethyldisilane, $(CH_3)_6Si_2$, appear to be analogous to those encountered in the present work and hence deserve comment. Fig. 14a shows the results of proton magnetic resonance in solid $(CH_3)_6Si_2$ [16]. The line-width in PMR is a measure of the order in the system. A decrease in line-width signifies increased disorder in the system. As a result, the variation of entropy with temperature (Fig. 14b) and hence the variation of dS/dT with temperature (Fig. 14c) can be qualitatively predicted from the temperature dependence of the line width observed in PMR studies. It is interesting to note that in the case of $(CH_3)_6\ Si_2$ also, the curve of dS/dT versus temperature exhibits a maximum and that this change has been attributed to the onset of internal rotation

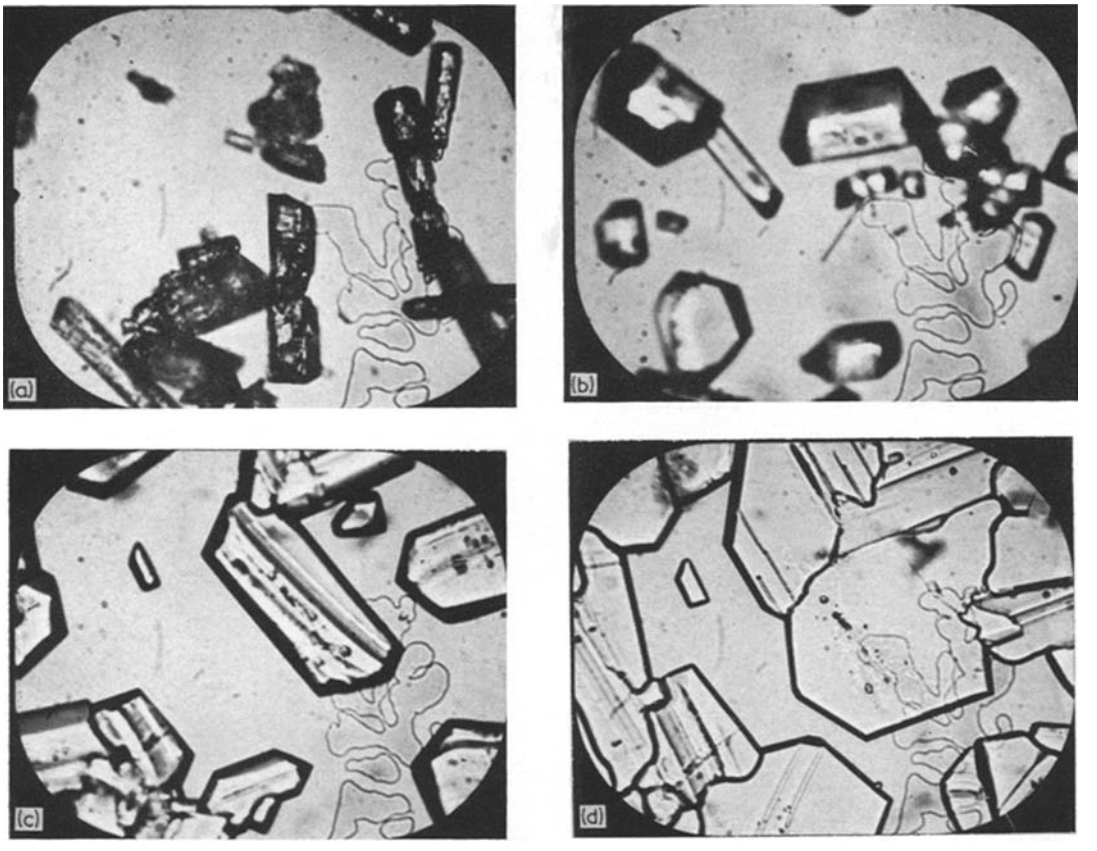

Figure 12 Optical micrographs of vapour-grown monomer crystals during heating: (a) room temperature, before heating; (b) 157° C; (c) 177° C, (d) 195° C.

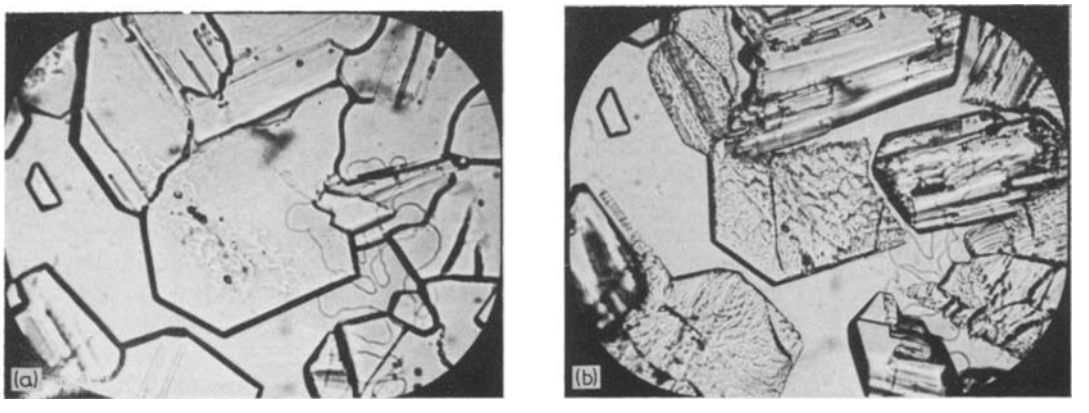

Figure 13 Optical micrographs of same vapour-grown monomer crystals as in Fig. 19, but here (a) at 190° C during cooling and (b) at room temperature after cooling.

around the Si-Si bond [16]. This then lends support to the explanation extended in the MMCT model.

It is speculated that in the case of trithiane, the proposed orientational phenomenon may involve one of the two modes of motion shown in Fig. 15. Fig. 15a depicts a conformational motion consisting of the co-ordinated flipping of the

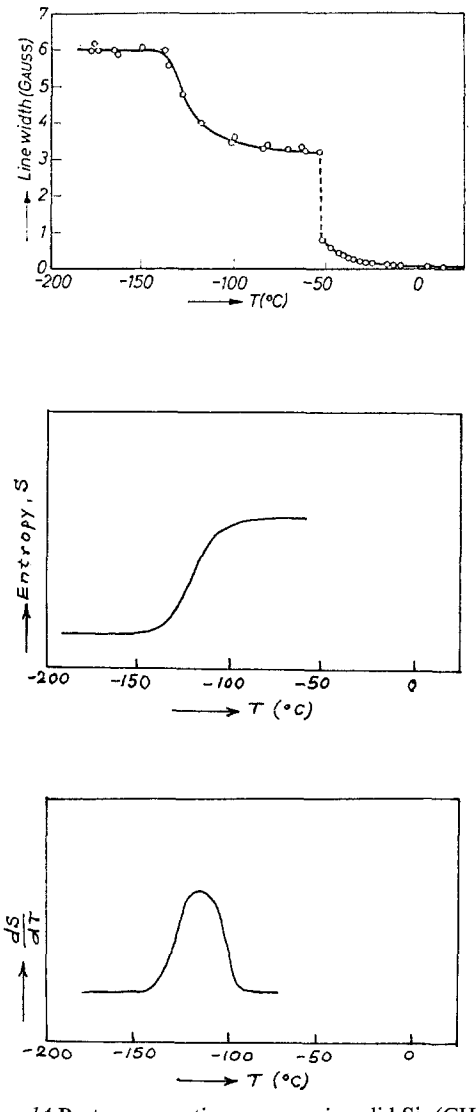

Figure 14 Proton magnetic resonance in solid $Si_2(CH_3)_6$.

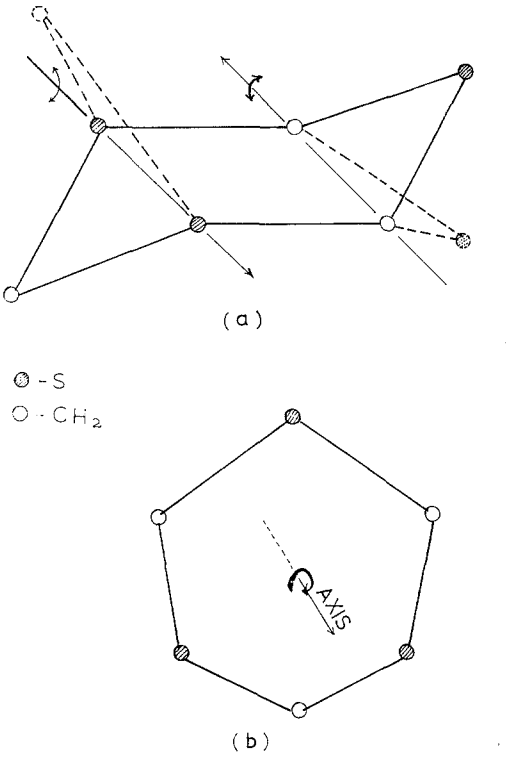

Figure 15 Possible internal modes of motion in trithiane.

two ends of the trithiane molecule in chair configuration. Fig. 15b illustrates a probable rotational motion of the molecule about the axis perpendicular to the plane of the paper.

It is known that solid-state polymerization reactions take place by an ionic-addition mechanism. Since the initiation step (γ-irradiation) is separated from the propagation and termination steps, in the study of post-irradiation polymerization, only the rates of propagation and termination need be considered. In the solid state, probably the most important factor governing the propagation step is the relative orientation of adjacent monomer molecules. As the temperature is increased, the unlocking of a conformational or rotational mode of motion tends to increase the probability of attaining the particular orientation favourable for the adjacent molecules to combine. This situation is schematically demonstrated in Fig. 16. The propogation step is thus sensitive to the frequency and amplitude of vibration in the solid state.

We may view the polymerization here as a competition between propagation and termination. The termination step in ionic radical polymerizations requires the rearrangement of an ion pair and thus involves an appreciable activation energy [18]. On the other hand, propagation would relate to interaction between neighbouring molecules. As depicted in Fig. 16, such processes would depend upon the degree of relative motion between lattice molecules in adjacent sites. We have seen that one such process apparently saturates near 175°C; as opposed to this saturation, the termination reaction exhibits an exponential dependence on temperature and is more pronounced at higher temperatures. Hence we should expect the rate of termination to overtake the propagation rate at a temper-

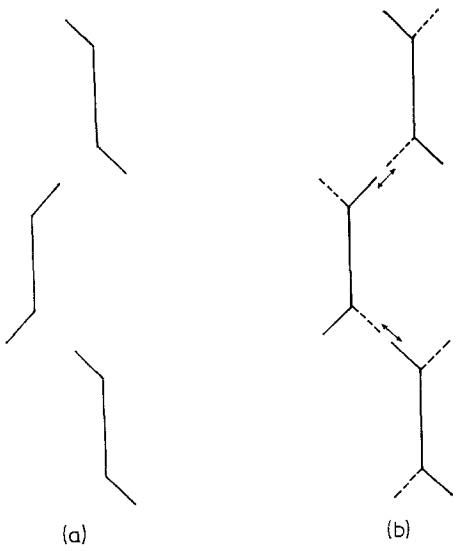

Figure 16 Propagation step in solid-state polymerization: (a) monomer molecules before orientational change, (b) monomer molecules after the onset of internal motion.

ature somewhere near the saturation temperature (175°C).

4.2. Unfavourable structure (US) model

An alternate explanation is based on a model in which molecules in the higher-temperature phase (phase I) packing begin to appear in the lower temperature phase II below the transition temperature and in which the proportion of molecules in phase I packing increases as the transition temperature is approached. Such a model would be consistent with either a second-order phase transition or with Boltzmann distribution of unstable phase I embryos in stable phase II (see, e.g. [19]). Examples of the coexistence of two structures over a temperature range have been reviewed by Ubbelohde [20].

In order to explain the polymerization data, it is necessary to postulate that either the propagation reaction is hindered or the termination rate is enhanced.

That there is some intimate connection between a phase transition and the polymerization rate of other solid-state polymerization reactions has been suggested previously [9, 21, 22]. ESR measurements have indicated that there is a direct correlation between crystal structure and the mobility of trapped radicals [21, 22]. However, in the previous instances, the exact placement of the polymerization-rate maximum relative to the transition temperature had not been well established, nor had the temperature correlation between rate of radical decay rate and the transition temperature. In the present investigation, it was seen that the polymerization rate peaked *below* the transition temperature. Hence, it has been necessary to conjecture that a precursory phase transition must occur. This type of model is nonetheless pleasing, because it could relate the rate of polymerization directly to details of the intermolecular organization on a crystal lattice rather than to a less-specific radical mobility.

Both of the above models tend to be somewhat unsettling, as they do not interlock. That is, the presence of the phase transition does not contribute to the MMCT model, nor does the saturation of a mode of motion below the phase transition temperature immediately augment the US model. It would be intellectually pleasing were a link to be found. Bowden and O'Donnell have proposed that the presumably "looser" structure of the higher-temperature phase would promote greater radical mobility and an enhanced termination rate. However, there is no existing data which explicitly isolates such a crystallographic effect from thermal effects. It appears that very careful and detailed experimentation will be required to satisfactorily answer the unsettled question in this area. Progress will be made only when data on (a) polymerization rate, (b) crystalline structure (including defect state), (c) radical concentrations, and (d) mobility of matrix and defect molecules are all available on a given system.

5. Conclusions

It is the opinion of the authors that the present work has raised many more questions than it has answered. Nonetheless, some "hard" conclusions can be drawn.

1. The rate of radiation-initiated polymerization of trithiane peaks at a temperature near 175°C.
2. The rate of change of entropy of the monomer phase with temperature also peaks near 175°C. This phenomenon is associated with the saturation of a mode of motion within the crystal.
3. A crystalline phase transition within the monomer occurs at a temperature near 194°C.
4. Solid-state polymerization studies which employ primarily one or a small number of tools are not likely to provide useful mechanistic information. It is essential that such problems be studied by a panoply of tools which will inter-

relate radical concentrations, crystal structure data (including static defects), mobility within the lattice, and the rate of polymerization.

Acknowledgements

We gratefully acknowledge the help of Mr James Prober with regard to differential thermal analysis. We are grateful also to Dr R. L. McCullough for a useful and productive discussion on possible physical models of the observed behaviour.

This work was supported by a grant from the National Science Foundation.

References

1. V. BUSETTI, M. MAMMI, and G. CARAZZOLO, *Z. Krist.* **119** (1963) 310.
2. G. CARAZZOLO, M. MAMMI, and G. VALLE, *Makromol. Chem.* **100** (1967) 295.
3. J. B. LANDO and V. STANNETT, *J. Polymer Sci.* **B-2** (1964) 375.
4. M. MAMMI, G. CARAZZOLO, G. VALLE, and A. DEL PRA, *Z. Krist.* **127** (1968) 401.
5. M. MAMMI, G. VALLE, and G. CARAZZOLO, *Nuovo Cimento* **53B** (1968) 73.
6. G. VALLE, G. CARAZZOLO, and M. MAMMI, *Ric. Sci.* **35** (II-A) (1965) 1469.
7. J. B. LANDO and V. STANNETT, *J. Polymer Sci.* **A-3** (1965) 2369.
8. M. MAMMI, G. CARRAZOLO and G. VALLE, *ibid* **B-3** (1965) 863.
9. S. OKAMURA, K. HAYASHI, and Y. KITANISHI, *ibid* **58** (1962) 927.
10. Y. TABATA, S. SHU, and K. OSHIMA, in "Organic Solid State Chemistry," ed. G. Adler (G. and B. Science Publishers, New York, 1969) p. 435.
11. J. M. SMITH and H. C. VAN NESS, "Introduction to Chemical Engineering Thermodynamics" (McGraw-Hill, New York, 1959).
12. H. NAUTA, *Phil. Mag.* **13** (1966) 1023.
13. N. F. VON MOERMAN and E. H. WIEBENGA, *Z. Krist.* **97** (1937) 323.
14. J. LAL, *J. Org. Chem.* **26** (1961) 971.
15. D. W. MCCLURE, *J. Chem. Phy.* **49(4)** (1968) 1830.
16. I. NITTA, *Z. Krist.* **122** (1959) 234.
17. Y. SAKAI and M. IWASAKI, *J. Polymer Sci.* **A1-7** (1969) 1749.
18. F. W. BILLMEYER, "Textbook of Polymer Science," (Wiley-Interscience, New York, 1971) p. 315.
19. J. FRENKEL, "Kinetic Theory of Liquids" (Oxford University Press, Fair Lawn, New Jersey, 1946).
20. A. R. UBBELOHDE, *Brit. J. Appl. Phys.* **7** (1956) 313.
21. Y. SAKAI and M. IWASAKI, *J. Polymer Sci.* **A1-7** (1969) 3143.
22. M. J. BOWDEN and J. H. O'DONNELL, *ibid* **A1-7** (1969) 1657.

Received 17 March and accepted 25 September 1972.